

✂ Author's Choice

Stable Isotope Labeling by Amino Acids in Cell Culture and Differential Plasma Membrane Proteome Quantitation Identify New Substrates for the MARCH9 Transmembrane E3 Ligase*[§]

Simon Hörz[‡], Tamar Ziv[§], Arie Admon[§], and Paul J. Lehner^{‡¶}

The regulation of cell surface receptor expression is essential for immune cell differentiation and function. At the plasma membrane ubiquitination is an important post-translational mechanism for regulating expression of a wide range of surface proteins. MARCH9, a member of the RING-CH family of transmembrane E3 ubiquitin ligases, down-regulates CD4, major histocompatibility complex-I (MHC), and ICAM-1 in lymphoid cells. To identify novel MARCH9 substrates, we used high throughput flow cytometry and quantitative mass spectrometry by stable isotope labeling by amino acids in cell culture (SILAC) to determine the differential expression of plasma membrane proteins in a MARCH9-expressing B cell line. This combined approach identified 13 potential new MARCH9 targets. All of the SILAC-identified targets for which antibodies were available were subsequently confirmed by flow cytometry, validating the proteomics results. A close correlation ($r^2 = 0.93$) between -fold down-regulation as determined by SILAC and flow cytometry was found, with no false positive hits detected. The potential new MARCH9 substrates cover a wide range of functions and include receptor-type protein-tyrosine phosphatases (e.g. PTPRJ/CD148) as well as Fc γ receptor IIB (CD32B), HLA-DQ, signaling lymphocytic activation molecule (CD150), and polio virus receptor (CD155). The identification of plasma membrane targets by SILAC with confirmation by flow cytometry represents a novel and powerful approach to analyze changes in the plasma membrane proteome. *Molecular & Cellular Proteomics* 8: 1959–1971, 2009.

The regulation of cell surface receptors is essential for the maintenance of cell homeostasis and intercellular communication. At the plasma membrane ubiquitination has emerged as a critical post-translational mechanism for regulating expression of a wide range of surface proteins, including recep-

tors of the immune system (1, 2). The plasma membrane of immune cells hosts housekeeping receptors such as amino acid and ion transporters as well as a diverse range of proteins tailored to immune function. These include receptors for cellular and soluble ligands, antigen-presenting molecules, and adhesion molecules as well as cell-specific receptors such as NK¹ cell, T cell, and B cell receptor complexes. 350 cluster of differentiation (CD) molecules have been defined by monoclonal antibodies raised against cell surface proteins, and many of these are exclusive to lymphocytes (3). The prominent role of transmembrane proteins in cellular function is emphasized by the observation that ~20% of the genome codes for proteins with at least one hydrophobic α helix (4).

The ability of receptors at the cell surface to respond to ligand stimulation is particularly important when the duration and intensity of signaling must be limited. The expression of cell surface proteins therefore undergoes constant turnover by endocytosis and recycling. For example the constitutively recycling T cell receptor is ubiquitinated and degraded following receptor stimulation (5). Endocytosed membrane proteins either recycle back to the plasma membrane or are degraded. The conjugation of ubiquitin to a receptor leads to the recruitment of ubiquitin-binding proteins, adaptors that mediate

¹ The abbreviations used are: NK, natural killer; CIITA, MHC class II transactivator encoded by the gene AIR-1 (activator of immune response locus 1); CD, cluster of differentiation; EGFR, epidermal growth factor receptor; Fc γ R, Fc γ receptor; GFP, green fluorescent protein; HLA, human leukocyte antigen; ICAM, intercellular adhesion molecule; Ig, immunoglobulin; MARCH, membrane-associated RING-CH; MHC, major histocompatibility complex; PTPR, protein-tyrosine phosphatase, receptor type; PVR, polio virus receptor; RING, really interesting new gene; RING-CH, variant RING domain, structurally related; SAP, SLAM-associated protein, also named SH2D1A; SH3BP1, Abl-SH3 domain-binding protein; SILAC, stable isotope labeling by amino acids in cell culture; SLAM, signaling lymphocytic activation molecule, also CD150; VAMP, vesicle-associated membrane protein; E1, ubiquitin-activating enzyme; E2, ubiquitin carrier protein; E3, ubiquitin-protein isopeptide ligase; APC, allophycocyanin; Bis-Tris, 2-[bis(2-hydroxyethyl)amino]-2-(hydroxymethyl)propane-1,3-diol; ABC, ammonium bicarbonate; LTQ, linear trap quadrupole; HA, hemagglutinin; Endo H, endoglycosidase H; siRNA, short interfering RNA; LIR, leukocyte immunoglobulin-like receptor; ER, endoplasmic reticulum; ESCRT, endosomal sorting complex required for transport; H, heavy; L, light.

From the [‡]Cambridge Institute for Medical Research, University of Cambridge, Cambridge CB2 0XY, United Kingdom and [§]Department of Biology, Technion-Israel Institute of Technology, Haifa 32000, Israel

✂ Author's Choice—Final version full access.

Received, April 1, 2009, and in revised form, May 13, 2009

Published, MCP Papers in Press, May 20, 2009, DOI 10.1074/mcp.M900174-MCP200

transport of the substrate to the proteasome or lysosome for degradation. The ubiquitination cascade requires monomeric ubiquitin to be activated by the ubiquitin E1 enzyme, transferred to one of ~40 E2 ubiquitin conjugases, and targeted to the acceptor residue, usually a lysine, of the target protein. This last reaction is catalyzed by one of around 400 ubiquitin E3 ligases that associate with the substrate and thus confer specificity to the ubiquitin reaction (6). The ligases are therefore the critical components of the reaction. The receptor tyrosine kinases were the first mammalian receptors shown to be ubiquitinated in a ligand-dependent manner (7, 8). Upon ligand binding the receptor tyrosine kinase is autophosphorylated, leading to recruitment of Cbl, a RING-type E3 ligase, which results in receptor ubiquitination, internalization, and lysosomal degradation. Mutation of the ubiquitin-targeted lysine residues in the cytoplasmic tail of the epidermal growth factor receptor (EGFR) prevents degradation and partially restores surface expression (9). Conversely overexpression of Cbl leads to reduced surface expression and ubiquitination of EGFR (10).

The membrane-associated RING-CH (MARCH) E3 ligases are a subfamily of the RING E3 ligases (11). Originally identified by viral E3 ligases involved in γ -herpesvirus immunoevasion, the defining feature of this family is the presence of a RING-CH domain, a modification of the zinc-binding module seen in classical RING E3 ligases, which is essential for recruitment of the E2 ubiquitin-conjugating enzyme (12). The RING-CH family is characterized by an unusual spacing of the metal-binding ligands in the C_4HC_3 orientation as opposed to the more common C_3HC_4 arrangement, and the majority of family members contain two transmembrane domains connected by a short extracellular loop. The canonical members of this group, the K3 and K5 viral E3 ligases of Kaposi sarcoma-associated herpesvirus, down-regulate a number of critical immunoreceptors (13, 14). In contrast, substrates of the 11 cellular MARCH proteins remain only partially characterized (11), but two MARCH proteins, MARCH1 and MARCH8, down-regulate MHC class II molecules as well as CD86 expressed on antigen-presenting cells including dendritic cells and B cells (15, 16).

MARCH9 is predominantly expressed in B and T lymphocytes as well as dendritic cells (Genomics Institute of the Novartis Research Foundation SymAtlas (17)). Three potential MARCH9 substrates have been identified as overexpression of MARCH9 leads to down-regulation of CD4 and MHC class I molecules (11) as well as ICAM-1 (18). Because MARCH9 down-regulates three cell surface receptors of a limited number examined, we hypothesized that MARCH9 is likely to have additional substrates. However, identifying the substrates of E3 ligases remains challenging. The interaction between a ligase and its substrate is transient and difficult to trap, particularly so for integral membrane proteins as with MARCH9 and its potential substrates. We therefore chose to compare the cell surface expression of proteins in the presence and absence of MARCH9. Although this approach cannot prove

whether a differentially expressed cell surface protein is a direct or indirect target for MARCH9, it does give a preliminary guide to the identification of potential substrates.

In this report we describe two approaches to analyze the effects of MARCH9 expression in a human B cell line. These include (i) high throughput flow cytometry using a panel of antibodies for proteins expressed on B cells and (ii) quantitative mass spectrometry of the plasma membrane proteome. Flow cytometry has the advantage of rapidly yielding quantitative data for those surface molecules where suitable and well characterized antibodies are available. In contrast, mass spectrometry allows a more objective comparison of the relative abundance of proteins between different cell types. We used stable isotope labeling by amino acids in cell culture (SILAC) (19) and looked for differentially expressed proteins from enriched plasma membranes of B cells overexpressing the MARCH9 E3 ligase. The mass spectrometry approach identified 12 potential MARCH9 substrates, six of which were subsequently confirmed by flow cytometry. Taken together our results demonstrate that the combined approach of flow cytometry and mass spectrometry provides a powerful way for identifying differentially regulated cell surface proteins and suggest an important role for MARCH9 in the regulation of lymphocyte function.

EXPERIMENTAL PROCEDURES

Antibodies—Most antibodies were unconjugated mouse monoclonal antibodies from Caltag Laboratories except for membrane IgD (Sigma); CD32-APC, CD54-APC, and CD166 (BD Biosciences); CD148 (MBL International Corp.); CD150 (eBioscience); CD155 (NeoMarkers); and HLA-DP and -DQ (BioLegend). MHC-I was a W6/32 hybridoma supernatant. Secondary anti-mouse antibody, cross-absorbed against other species and Cy5-conjugated, was from Jackson ImmunoResearch Laboratories. Human immunoglobulin to block Fc receptors was from Sigma.

Lentiviral Transduction—MARCH9 was cloned into pHR SIN Ub emerald (expressing the green fluorescent protein emerald under control of the ubiquitin promoter) (a kind gift from Yasuhiro Ikeda) and co-transfected into 293T cells together with pMD-G (encoding the vesicular stomatitis virus G envelope protein) and pCMV8.91 (encoding the gag-pol fusion protein) at equimolar ratios to generate viral particles. Supernatants were filtrated through 0.45- μ m membranes, and virus was precipitated by ultracentrifugation at $100,000 \times g$. Concentrated virus was used to transduce the Epstein-Barr virus-positive Burkitt lymphoma B cell line Hs-Sultan (a kind gift from Zou Xiang; ATCC CRL-1484) to generate Sultan-MARCH9 cells. Transduction efficiency was ~50%. No highly GFP-positive cells were generated even after a second round of transduction; this is probably due to toxic effects of highly overexpressed MARCH9. We used the untransduced population as an internal control in the flow cytometry screen, whereas for isotope labeling the cells were sorted for GFP expression to exclude untransduced cells. Sultan-GFP control cells only expressing GFP were generated with virus derived from GFP-expressing pHR SIN-GFP Ub emerald.

High Throughput Flow Cytometry—Cells were washed in PBS, and Fc receptors were blocked with human IgG (50 μ g/ml) for 15 min on ice. 5×10^4 cells/well were labeled in 96-well plates with either APC-conjugated or unconjugated antibody followed by Cy5-conjugated secondary antibody on ice in the presence of human IgG.

Antibody staining was analyzed on a FACSCalibur with high throughput plate loader (BD Biosciences). Data were analyzed with FlowJo (Tree Star) and gated for the live cell population. Any further gating is indicated in the figures.

SILAC—Sultan-MARCH9 cells were grown in lysine- and arginine-free RPMI 1640 medium (Thermo Scientific) with 10% dialyzed FCS (JRH Biosciences) supplemented with isotope-labeled “heavy” [$^{13}\text{C}_6$, $^{15}\text{N}_2$]lysine (Lys8) and [$^{13}\text{C}_6$, $^{15}\text{N}_4$]arginine (Arg10) (100 $\mu\text{g}/\text{ml}$; Cambridge Isotope Laboratories), whereas Sultan-GFP cells were grown with normal “light” amino acids. The cells underwent at least seven cell divisions with medium changes every day to minimize cell death. Both cell lines divided at a similar rate.

Plasma Membrane Purification—The plasma membrane purification was performed using the cationic silica microbead isolation procedure (20) with modifications as described previously (21). Briefly 2×10^8 labeled Sultan-MARCH9 and Sultan-GFP cells were pooled and coated with cationic silica beads (Ludox-CL, Sigma), washed, and cross-linked with polyacrylic acid. The coated cells were incubated in hypotonic buffer and lysed by nitrogen cavitation (Cell Disruption Bomb, Parr Instrument Co.). The silica-coated plasma membrane fragments were then purified twice by sedimentation through a 70% Histodenz cushion. The pellet was washed three times with lysis buffer and five times with 0.1 M Na_2CO_3 . Membrane proteins were extracted directly in SDS sample buffer, separated on a precast 4–12% Bis-Tris gel (Invitrogen), and Coomassie Blue-stained.

In-gel Proteolysis and Mass Spectrometry Analysis—The lane was cut into 10 slices that were washed with 100 mM ammonium bicarbonate (ABC). The proteins in the gel were reduced with 10 mM DTT at 60 °C for 30 min and alkylated with 10 mM iodoacetamide at room temperature for 30 min. The bands were washed with 50 mM ABC, 50% ACN solution and dehydrated with 100% ACN. The proteins were proteolyzed “in gel” overnight at 37 °C using modified trypsin (Promega) at a 1:100 enzyme-to-substrate ratio in 10 mM ABC, 10% ACN. Supernatants were transferred to new tubes. The resulting peptides were resolved by on-line reversed phase nanoscale capillary LC and analyzed by electrospray MS/MS. Using a NanoLC-1D plus system (Eksigent), peptides were resolved by 0.075- μm -inner diameter capillaries of about 20-cm length (J&W) packed in house with 3- μm Reprosil reversed phase material (Dr. Maisch GmbH). The peptides were eluted with linear 90-min gradients of 5–45% and 15 min at 95% acetonitrile with 0.1% formic acid in water at flow rates of 0.25 $\mu\text{l}/\text{min}$. The LC setup was connected to an LTQ-Orbitrap mass spectrometer (Thermo Fisher Scientific) equipped with a nanoelectrospray ion source. Data-dependent acquisition was performed on the LTQ-Orbitrap using the Xcalibur 2.04 software. Mass spectrometry was performed in a positive mode using repetitive full MS scans followed by CID of the seven most dominant ions selected from the first MS scan. Each mass was excluded from the mass list for 30 s following its fragmentation.

The mass spectrometry data were analyzed using Sequest 3.31 software (including Extract_msn for peak list generation) (J. Eng and J. Yates, University of Washington and Thermo Finnigan, San Jose, CA) searching against the human part of the UniProt database (November 2007) including 27,564 proteins. The search was for tryptic peptides with two missed cleavage sites. The peptide tolerance was set to 50 ppm, and fragment ion tolerance was set to 0.5 Da. Carbamidomethylcysteine was set as a fixed modification, and oxidized methionine and the SILAC labels (Lys8 and Arg10) were searched as variable modifications. The MS data were filtered according to the XCorr (above 2.2 for doubly charged peptides, 2.8 for triply charged peptides, and 3 for quadruply charged peptides), peptide probability (<0.09), and accuracy (<15 ppm). Using this combination of filters resulted in a false positive rate of 0.98%. The false positive rate was calculated by dividing the number of identified peptides using the

reversed human UniProt database by the number of hits using the regular database.

The quantification was done using PepQuant (Thermo Fisher Scientific) to measure the peak area of each identified peptide at both heavy and light isotopes with a mass tolerance of 0.01 Da using combined scans. The H:L ratio of the protein was determined (by an in-house software tool) as an average of the ratio of its peptides excluding outlying peptides (more than 5-fold the average). Peptides that matched more than one protein were excluded from the quantification with the exceptions specified in the next paragraph.

Non-unique Peptides—MHC molecules are highly polymorphic in their peptide binding domains with areas of sequence conservation that result in peptides mapping to multiple allelic variants of the same gene. Where peptides did map to variants of the same gene we included those and grouped them into HLA-A, -B, -DP, -DQ, and -DR (no HLA-C-specific peptides were identified). In addition to their polymorphism the MHC class II molecules are also heterodimeric proteins, and we grouped peptides mapping to either chain into HLA-DP and -DR. We list the MS results for HLA-DQA and -DQB separately to show how both chains are affected. For confirmation by flow cytometry a pan-MHC class I antibody and HLA-DP, -DQ, or -DR group-specific antibodies were used.

ILT-2 (LIRB1) and the related ILT-4 (LIRB2) were both only identified by the same single peptide. B cells only express ILT-2, and the expression can be analyzed by flow cytometry with an ILT-2-specific antibody. Consequently we included ILT-2 in our screen.

All other protein identifications were based on unique peptides only. In cases where both heavy and light peptide were identified by MS/MS and therefore independently quantified, both quantifications were used to calculate the average change in expression.

Transient Transfection, Metabolic Labeling, and Pulse-Chase Analysis—293T cells were transfected with pcDNA3-based expression constructs for $\text{Fc}\gamma\text{RIIB}$ or SLAM and pEGFP constructs of wild-type and mutant MARCH9 using TransIT 293 reagent (Mirus). 24 h later the cells were starved for 1 h in methionine- and cysteine-free medium, labeled with [^{35}S]methionine and [^{35}S]cysteine (12 MBq/ml; Easy Tag labeling mixture, PerkinElmer Life Sciences) for 20 min, and chased in medium containing excess cold methionine and cysteine for the indicated time periods. The cells were lysed in 1% Triton X-100 and precleared twice with CL-4B Sepharose beads (Sigma-Aldrich), and HA-tagged SLAM was precipitated with the HA.11 monoclonal antibody (clone 16B12, Covance) and protein A-Sepharose for 1 h, washed three times with 0.5% Triton X-100 in PBS, eluted in sample buffer, and heated to 95 °C for 10 min. For endoglycosidase H (Endo H) digestion samples were supplemented with 250 units of Endo H (New England Biolabs) and incubated at 37 °C for 1 h.

RNA Interference—65 h preanalysis, 293T cells were transfected with RNA oligonucleotides specific for Tsg101 (40) in Oligofectamine (Invitrogen) at a concentration of 30 nM siRNA. 24 h preanalysis the same cells were transiently transfected with SLAM and GFP-tagged MARCH9 with TransIT 293 reagent (Mirus). SLAM expression was analyzed by flow cytometry with SLAM-specific antibodies (clone A12, BioLegend); GFP fluorescence was used to assess MARCH9 expression. Tsg101 knockdown was confirmed by Western blot with a Tsg101-specific antibody.

RESULTS

Identification of Novel MARCH9 Substrates Using a Flow Cytometry-based Screening Approach—As part of our initial attempt to identify novel targets down-regulated by the MARCH9 E3 ligase we used a panel of monoclonal antibodies to analyze the cell surface expression of 44 surface proteins by flow cytometry in MARCH9-overexpressing cells. Tran-

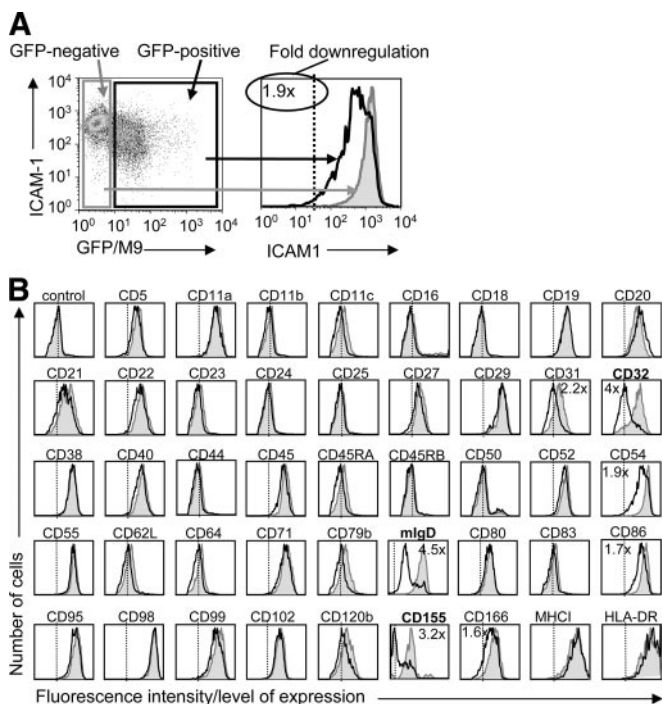


FIG. 1. Flow cytometry-based screen to identify novel MARCH9 substrates. A, Sultan MARCH9 B cells were generated by lentiviral transduction and co-expressed GFP from a separate promoter. The *black line* in the histogram represents the population gated for high expression of GFP, *i.e.* MARCH9-expressing; the *filled gray line* is the GFP-negative population; background levels are marked by the *vertical dotted line* that indicates the position of the peak of the control sample. B, surface expression of a panel of 44 B cell markers was compared between MARCH9-expressing cells and the untransduced GFP-negative population. The -fold reduction in mean fluorescence intensity is given for those samples that were repeatedly down-regulated. *mlgD*, membrane IgD.

scriptional profiles suggest MARCH9 is expressed in B and T lymphocytes as well as dendritic cells, and we therefore over-expressed MARCH9 in the Epstein-Barr virus-positive Burkitt lymphoma B cell line Hs-Sultan by lentiviral transduction. The available MARCH9-specific antibodies are not of sufficient sensitivity to detect endogenous MARCH9, and we were therefore unable to compare the expression levels of over-expressed and endogenous protein. The lentiviral vector also encodes GFP under a separate promoter, allowing ready identification of MARCH9-positive cells. MARCH9-transduced cells were stained with the specific antibodies in 96-well plates and analyzed by high throughput flow cytometry (Fig. 1). GFP-expressing control cells were stained in the identical way, and GFP did not affect expression levels of any surface marker (data not shown). As only 50% of the MARCH9-transduced Sultan cells expressed GFP, the GFP-negative population served as an internal control for steady state expression levels of each protein analyzed (Fig. 1A). Proteins detected at less than 3 times the background fluorescence were excluded from further analysis. 26 of 44 surface proteins analyzed were detected above this threshold

(Fig. 1B). As expected the ICAM-1 (CD54) adhesion molecule was targeted, leading to an approximate 2-fold reduction in mean fluorescence intensity in the MARCH9-expressing population, whereas MHC class I levels were not affected in these cells, confirming our previous results that MHC class I molecules do not appear to be especially good substrates for MARCH9 (18). We used ICAM-1 as our benchmark to assess the down-regulation observed for potential new targets of MARCH9. Three proteins previously identified as substrates of the Kaposi sarcoma-associated herpesvirus-encoded viral E3 ligase K5, platelet/endothelial cell adhesion molecule (CD31), B7.2 (CD86), and activated lymphocyte cell adhesion molecule (CD166), were also moderately down-regulated in the presence of MARCH9 comparably to or less than ICAM-1 (22). A much stronger effect of MARCH9 was seen on three novel targets: Fc γ RIIB (CD32B), membrane-bound IgD, and PVR (CD155). Fc γ RIIB, an inhibitory receptor for the Fc portion of antibodies, was reduced to background levels (indicated by the *dotted line*), whereas decreased expression of the central component of the B cell antigen receptor, membrane-bound IgD, was seen. Cell surface expression of the NK cell ligand PVR, which is down-regulated by the human cytomegalovirus (23), was reduced to background levels in MARCH9-expressing cells.

Identification of Novel MARCH9 Substrates Using SILAC and LC-MS/MS—The results from the flow cytometry-based screen were encouraging, but this approach is limited by the availability and prohibitive cost of antibodies required for cell surface screening. To gain a more extensive picture we took a plasma membrane proteomics approach using SILAC and mass spectrometry to compare levels of plasma membrane proteins between control and MARCH9-overexpressing cells. MARCH9-GFP-expressing cells and control GFP-expressing cells were sorted, and the MARCH9-expressing cells cultured in the presence of heavy isotope-labeled [$^{13}\text{C}_6$, $^{15}\text{N}_2$]Lys8 and [$^{13}\text{C}_6$, $^{15}\text{N}_4$]Arg10, whereas the control cells were grown in normal medium. After at least seven cell divisions the two cell populations were combined at equal cell numbers, and the plasma membrane was purified. Although the plasma membrane is a readily accessible compartment, it is difficult to separate from intracellular membranes and requires a significant enrichment as it contains only 2–3% of the total cell protein (21). We chose the cationic silica pellicle method (20) with the modifications described previously (21). This is a purely mechanical purification method and does not involve any modification of the plasma membrane proteins (Fig. 2). The cell surface is coated with cationic silica beads, which are then cross-linked and neutralized with polyacrylic acid before the cells are lysed by nitrogen cavitation. The plasma membrane stays attached to the silica shell, allowing purification on a Histodenz density gradient and extensive washing with carbonate buffer to minimize contamination with cytosolic and nuclear proteins. Membrane proteins are then eluted with SDS loading buffer and separated on a precast gel.

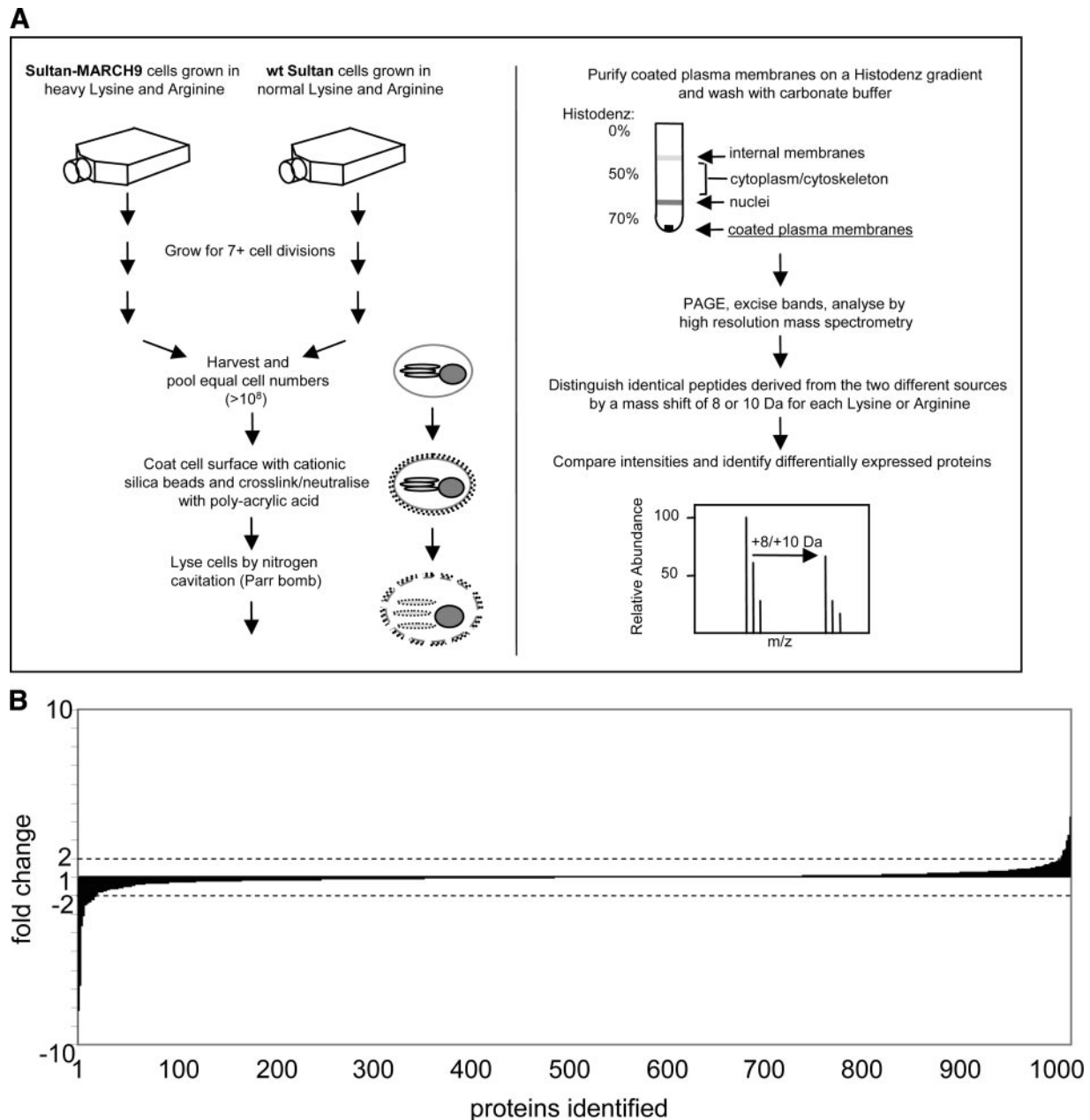


FIG. 2. Stable isotope labeling and plasma membrane preparation. *A*, Sultan B cells stably expressing MARCH9 were grown in medium only containing heavy arginine and lysine. After seven cell divisions equal cell numbers were pooled with control Sultan B cells grown in normal medium. The plasma membranes were purified with the pellicle method of Chaney and Jacobson (20), and the membrane proteins were eluted with SDS loading buffer. The protein mixture was separated on a precast SDS gel, divided into 10 pieces, tryptically digested, and analyzed by LC-MS/MS with an Orbitrap mass spectrometer. *B*, relative expression of all identified proteins plotted as a $-$ fold change. Negative values indicate a down-regulation in the presence of MARCH9. The cutoff for a 2-fold change is indicated by the dotted line. The ratio of all proteins identified was 1:1.02 with a standard deviation of 0.31. *wt*, wild type.

Using this approach we quantified just under 1000 proteins (1017 but with 23 multiple hits for polymorphic MHC molecules) of which 157 were plasma membrane proteins including 19 of the 26 identified by flow cytometry (Table I). Based on our experience with whole cell lysates from B lymphocytes where plasma membrane proteins only make up around 1.5% of the total, we estimate an \sim 10-fold enrichment. The occur-

rence of mitochondrial and nuclear proteins could be due to a small number of apoptotic or broken cells being coated with silica, resulting in a contamination with internal organelles. Our aim was to identify candidate proteins that are strongly down-regulated in the presence of MARCH9 and therefore represent potential novel substrates. Based on our flow cytometry results as well as the experience of other groups

TABLE I
Differential expression levels of plasma membrane proteins

Proteins down-regulated 2-fold or more are printed in bold; L:H gives the protein ratios of control to MARCH9-expressing cells; TM gives the number of transmembrane regions with "Lipid" indicating a lipid anchor, GPI indicating a glycosylphosphatidylinositol anchor, and "Peri" indicating a peripheral membrane protein; H:L is the protein ratio of MARCH9 to control cells; S.D. is the standard deviation of this ratio; coverage gives the percentage of precursor protein covered by peptides analyzed; UniProt accession numbers are given; "Pep" is the number of unique peptides used for identification, and "quant" is the number of independently quantified peptides used to calculate the H:L ratio and S.D.; underlined proteins were previously examined by flow cytometry. NA, not applicable. LDLR, low density lipoprotein receptor; PODXL, podocalyxin-like; FLVCR, feline leukemia virus subgroup C cellular receptor; LCAP, lung carcinoma-associated protein; LSR, lipolysis stimulated lipoprotein receptor; PAF, platelet-activating factor; LCK, lymphocyte-specific protein tyrosine kinase; NCSTN, nicastrin and CYBB, cytochrome b-245 heavy chain.

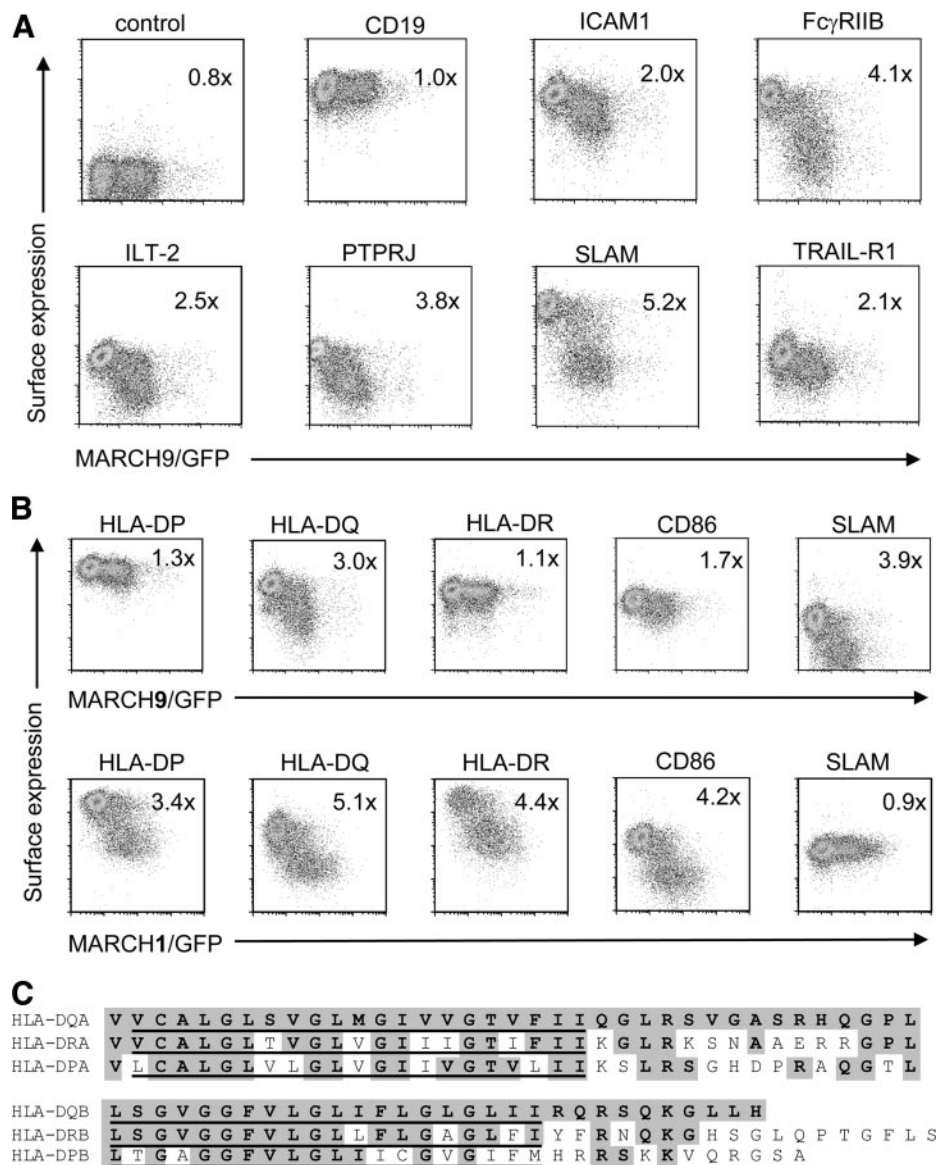
No.	Gene	L:H	TM	H:L	S.D. H:L	Coverage	UniProt	Pep (quant)	No.	Gene	L:H	TM	H:L	S.D. H:L	Coverage	UniProt	Pep (quant)
1	<i>PTPRA</i>	8.18	1	0.12	0.05	11.97	P18433	6 (6)	41	<i>MPZL1</i>	1.18	1	0.85	0.04	12.60	O95297	4 (6)
	<i>SLAM (CD150)</i>	4.73	1	0.21	0.08	9.85	Q13291	3 (4)		<i>KCP2^a</i>	1.18	4	0.85	0.00	10.50	Q8NGL1	1 (2)
	<i>FC-γRIIb (CD32B)</i>	3.65	1	0.27	0.02	12.30	P31994	2 (2)		<i>ATP1B3 (CD298)</i>	1.18	1	0.85	0.29	36.60	P54709	17 (20)
	<i>PTPRJ (CD148)</i>	3.22	1	0.31	0.08	14.44	Q12913	17 (24)		<i>HLA-DR</i>	1.18	1	0.85	0.27	40.60	P01903	30 (57)
	<i>HLA-DQB</i>	2.50	1	0.40	0.08	22.20	P03992	12 (15)		<i>JAM1</i>	1.17	1	0.85	0.05	7.40	Q9Y624	2 (3)
	<i>PTPRF^a</i>	2.46	1	0.41	NA	1.48	P10586	1 (1)		<i>SLC7A5 (CD98c)</i>	1.17	12	0.85	0.05	11.80	Q01650	2 (5)
	<i>VAMP8</i>	2.36	1	0.42	0.11	41.00	Q9BV40	6 (7)		<i>Syntaxin6</i>	1.17	1	0.86	0.07	14.10	O43752	2 (2)
	<i>ICAM (CD54)</i>	2.34	1	0.43	0.15	13.35	P05362	7 (6)		<i>MARCS2^a</i>	1.17	Lipid	0.86	0.07	7.83	P29966	2 (3)
	<i>ILT-2 (CD85)</i>	2.25	1	0.45	0.08	6.77	Q8NHL6	3 (2)		<i>SLC12A2</i>	1.16	12	0.86	0.20	12.29	P55011	10 (16)
	<i>TMEM2</i>	2.23	1	0.45	0.01	1.88	Q9UHN6	2 (2)	50	<i>SLCO3A1^a</i>	1.16	12	0.86	0.00	1.55	Q9UJG8	1 (2)
10	HLA-DQA	2.11	1	0.47	0.03	12.20	P01907	5 (7)		<i>CD316</i>	1.15	1	0.87	0.29	14.03	Q969P0	7 (10)
	Plexin C1 (CD232)	2.05	1	0.49	0.20	3.44	O60486	4 (5)		<i>EDG5</i>	1.15	7	0.87	NA	7.90	O95136	2 (1)
	<i>FCRL2</i>	1.96	1	0.51	0.02	4.53	Q96LA5	2 (2)		<i>SLC4A7</i>	1.15	11	0.87	0.17	3.95	Q9Y6M7	3 (5)
	<i>LDLR</i>	1.90	1	0.53	0.44	3.14	P01130	2 (3)		<i>NRP2</i>	1.14	1	0.87	0.34	5.91	O60462	4 (7)
	<i>MARCKSL1</i>	1.83	Lipid	0.55	0.36	51.30	P49006	4 (4)		<i>ATP13A3</i>	1.13	10	0.88	0.31	4.42	Q9H7F0	4 (4)
	<i>PODXL^a</i>	1.82	1	0.55	0.00	2.27	O00592	1 (2)		<u><i>PTPRC (CD45)</i></u>	1.13	12	0.88	0.24	27.84	P08575	41 (55)
	<i>TRAIL-R1 (CD261)</i>	1.80	1	0.56	0.00	2.10	O00220	1 (2)		<i>CD55</i>	1.13	GPI	0.89	0.07	10.24	P08174	3 (2)
	Ig μ chain	1.72	1	0.58	0.26	10.68	P01871	4 (6)		<i>SLC43A1/LAT3</i>	1.12	12	0.89	0.10	3.67	O75387	2 (3)
	<i>LAT2</i>	1.70	1	0.59	0.23	12.80	Q9GZY6	2 (4)	60	<i>Tetraspanin14</i>	1.12	4	0.89	0.06	14.10	Q8NG11	3 (4)
	<i>LRRC32^a</i>	1.68	1	0.60	0.00	2.72	Q14392	1 (2)		<i>CD70</i>	1.12	1	0.89	0.14	20.21	P32970	6 (10)
20	<i>TNFSF9^a</i>	1.58	1	0.63	0.00	6.70	P41273	1 (2)		<i>PTPRS</i>	1.12	1	0.89	0.19	9.29	Q13332	11 (17)
	Integrin β7 ^a	1.51	1	0.66	0.00	1.38	P26010	1 (2)		<i>RAB14</i>	1.11	Lipid	0.90	0.21	45.60	P61106	7 (11)
	<i>B7.2 (CD86)^a</i>	1.50	1	0.66	0.06	3.34	P42081	1 (2)		<i>SLC16A7/MOT2^a</i>	1.10	12	0.91	0.14	3.14	O60669	1 (7)
	<i>BMPRIA^a</i>	1.39	1	0.72	NA	2.82	P36894	1 (1)		<i>HLA-B</i>	1.10	1	0.91	0.15	46.90	P01889	11 (19)
	Lymphotoxin B	1.36	1	0.74	0.04	21.70	Q06643	2 (3)		<i>CD147</i>	1.10	1	0.91	0.26	25.71	P35613	7 (16)
	<i>SLC5A6</i>	1.35	13	0.74	0.02	4.72	Q9Y289	2 (4)		<i>Stomatin</i>	1.09	1	0.92	0.11	17.00	P27105	3 (5)
	<i>CD180</i>	1.32	1	0.76	0.12	15.28	Q99467	6 (7)		<i>ATP7A^a</i>	1.09	8	0.92	0.00	1.40	Q04656	1 (2)
	<i>SNAP29</i>	1.31	0	0.76	0.05	8.10	O95721	2 (2)		<i>RGS19</i>	1.09	Lipid	0.92	0.00	12.40	P49795	2 (2)
	<i>SLAMF5 (CD84)</i>	1.29	1	0.77	0.19	30.14	Q9UIB8	8 (10)		<i>SLC1A1</i>	1.08	10	0.93	0.33	6.68	P43005	2 (4)
	<i>FLVCR^a</i>	1.27	12	0.79	0.00	16.67	Q99808	7 (12)	70	<i>Presenilin</i>	1.08	8	0.93	0.08	8.10	P49768	2 (4)
30	<i>SLC29A1</i>	1.27	12	0.82	0.26	12.40	P53985	9 (16)		<i>CD19</i>	1.06	1	0.94	0.21	17.57	Q86X29	9 (16)
	<i>SLC16A1</i>	1.22	12	0.82	0.26	12.40	P53985	9 (16)		<i>LSR</i>	1.06	1	0.94	0.21	17.57	Q86X29	9 (16)
	<i>QR2 (CD21)</i>	1.22	1	0.82	0.23	7.84	P20023	7 (9)		<i>HLA-DP</i>	1.06	1	0.94	0.14	18.60	P04440	3 (6)
	<i>CKLF-6</i>	1.21	3	0.83	0.20	11.50	Q9NX76	2 (4)		<i>NCKKAP1L</i>	1.06	1	0.94	0.16	3.82	P55160	3 (4)
	<i>LCAP</i>	1.20	1	0.83	0.30	13.17	Q9UIQ6	9 (18)		<i>AT2B1/IPMCA1</i>	1.06	10	0.95	0.22	21.62	P20020	31 (37)
	<i>ADAM10</i>	1.19	1	0.84	0.22	16.98	O14672	9 (10)		<i>TMN33</i>	1.05	3	0.95	0.04	8.90	P57088	2 (2)
	<i>CD99^a</i>	1.19	1	0.84	0.07	5.40	P14209	1 (2)		<i>EVI2A^a</i>	1.05	1	0.95	0.35	8.19	P22794	1 (4)
	<i>CD10</i>	1.19	1	0.84	0.09	10.27	P08473	8 (12)		<i>SLC19A1</i>	1.05	12	0.95	0.17	12.18	P41440	5 (7)
	<i>SLAMF6</i>	1.19	1	0.84	0.10	5.70	Q96DU3	2 (3)		<i>SLC1A5</i>	1.05	10	0.95	0.39	32.35	Q15758	19 (34)
	<i>NKG2D</i>	1.18	1	0.84	0.11	10.20	P26718	2 (2)	80	<i>AT2B4/IPMCA4</i>	1.05	10	0.96	0.11	5.32	P23634	7 (10)

TABLE 1—Continued

No.	Gene	L:H	TM	H:L	S.D.	H:L	Coverage	UniProt	Pep (quant)	No.	Gene	L:H	TM	H:L	S.D.	H:L	Coverage	UniProt	Pep (quant)
81	SLC3A2 (CD98hc)	1.04	1	0.96	0.42	0.96	43.10	P08195	31 (37)	121	SLC2A5	0.93	12	1.07	0.25	13.57	P22732	10 (18)	
	EV12B	1.04	1	0.96	0.28	0.93	11.83	P34910	3 (6)		SLC2A1	0.93	12	1.08	0.30	15.24	P11166	8 (14)	
	CD58	1.04	1	0.96	0.05	0.93	4.80	P19256	2 (4)		SLC4A2	0.93	10	1.08	0.30	4.27	P04920	5 (5)	
	CyclinM4 ^a	1.03	5	0.97	0.00	0.93	2.19	G6P4Q7	1 (2)		REEF5 ^a	0.93	2	1.08	0.08	6.30	Q00765	1 (2)	
	SLC1A4	1.03	9	0.97	0.20	0.93	27.07	P43007	9 (17)		SCAMP2	0.93	4	1.08	0.14	10.00	O15127	2 (2)	
	CD22	1.02	1	0.98	0.21	0.92	12.51	P20273	9 (11)		VAMP3 ^a	0.92	1	1.09	0.04	16.00	Q15836	1 (4)	
	LCK	1.02	Lipid	0.98	0.26	0.92	31.24	P06239	11 (22)		SLC43A3	0.92	12	1.09	0.09	6.30	Q8NB15	4 (5)	
	Flotillin2	1.02	0	0.98	0.22	0.92	57.30	Q14254	29 (45)		MRP1/ABCC1	0.92	17	1.09	0.22	15.09	P33527	17 (24)	
	CD49d	1.01	1	0.99	0.29	0.92	12.14	P13612	10 (13)		CD100	0.92	1	1.09	0.12	18.33	Q92854	10 (10)	
	CD95	1.01	1	0.99	0.18	0.91	17.00	P25445	4 (7)	130	VAMP2	0.91	1	1.10	0.10	15.30	P63027	2 (3)	
	ATP1A3	1.01	10	0.99	0.14	0.91	5.82	P13637	6 (8)		CD47	0.91	5	1.10	0.15	8.70	Q08722	11 (10)	
	HLA-A	1.01	1	0.99	0.47	0.90	46.00	P30443	17 (22)		CD48	0.90	GPI	1.11	0.16	28.80	P09326	7 (14)	
	SNAP23	1.01	Peri	0.99	0.16	0.89	69.20	O00161	11 (17)		CLDN1	0.89	4	1.12	0.07	13.40	Q9NY35	3 (5)	
	NCSTN	1.00	1	1.00	0.04	0.89	3.24	Q92542	2 (4)		CD74	0.89	1	1.12	0.16	16.20	P04233	8 (10)	
CYBB	1.00	6	1.00	0.19	0.88	13.68	P04839	7 (12)		CD166	0.88	1	1.13	0.18	16.12	Q13740	5 (6)		
Plexin B2	1.00	1	1.00	0.16	0.87	22.36	O15031	33 (47)		Synaptogyrin	0.87	4	1.15	0.33	8.90	O43760	2 (2)		
CD63	1.00	4	1.00	0.08	0.86	5.04	P08962	4 (5)		CD38	0.86	1	1.16	0.46	38.00	P28907	9 (13)		
Vanin2	1.00	GPI	1.00	0.02	0.86	6.54	O95498	2 (3)		SLC25A5	0.86	6	1.16	0.31	16.40	P05141	4 (6)		
GNA11	0.99	0	1.01	0.09	0.86	9.50	P29992	2 (5)		ATP1A1	0.86	10	1.17	1.25	44.57	P05023	65 (78)		
CD81	0.99	4	1.01	0.07	0.85	26.27	P60033	8 (13)	140	CD18	0.85	1	1.17	0.39	37.71	P05107	30 (41)		
SCARB1 (CD36L1)	0.99	2	1.01	0.06	0.85	7.61	Q8WTV0	4 (5)		SYPL1	0.85	4	1.18	0.15	10.04	Q16563	2 (3)		
Syntaxin8	0.99	1	1.01	0.25	0.84	14.80	Q9UNK0	2 (2)		SIT1	0.84	1	1.18	0.48	39.80	Q9Y3P8	5 (6)		
MRP4/ABCC4	0.99	14	1.01	0.15	0.83	8.08	O15439	8 (11)		PLSCR1 ^a	0.83	1	1.20	0.52	6.30	O15162	1 (2)		
CD97	0.99	7	1.02	1.06	0.82	8.74	P48960	7 (12)		Syntaxin7	0.82	1	1.21	0.56	54.00	O15400	8 (14)		
ICAM2 (CD102)	0.98	1	1.02	0.12	0.82	17.45	P13598	4 (9)		CD20	0.82	4	1.21	0.34	34.00	P11836	15 (25)		
CD42	0.98	Lipid	1.02	0.12	0.82	11.00	Q17031	2 (3)		CD72	0.82	1	1.22	0.37	31.80	P21854	7 (13)		
PAG1	0.98	1	1.02	0.17	0.81	47.22	Q9NWQ8	17 (25)		CD37	0.81	4	1.23	0.36	19.93	P11049	7 (9)		
BASPTP	0.98	Lipid	1.02	0.15	0.81	30.84	P80723	4 (5)		CD45-AP	0.81	1	1.24	1.12	46.10	Q14761	9 (10)		
PAF receptor	0.97	7	1.03	0.20	0.80	12.57	P25105	4 (6)		Embrigin	0.80	1	1.26	0.27	29.36	Q6PCB8	5 (8)		
SLC44A1 (OD92)	0.97	10	1.03	0.26	0.78	13.24	Q8WMI5	4 (8)	150	CD11a	0.78	1	1.28	0.70	27.52	P20701	36 (46)		
SEM4A	0.97	1	1.04	0.37	0.78	16.03	Q9H3S1	8 (9)		CD275	0.78	1	1.28	0.37	7.62	O75144	2 (4)		
Ratfilin	0.96	Lipid	1.04	0.21	0.77	53.29	Q14699	21 (32)		CD79a ^a	0.77	1	1.30	0.00	9.70	P11912	1 (2)		
Integrin β5 ^a	0.96	1	1.04	NA	0.76	2.88	P18084	1 (1)		SLC44A2	0.76	10	1.32	0.22	6.52	Q8IWA5	4 (6)		
CD71	0.96	1	1.04	0.14	0.73	33.03	P02786	25 (33)		CD53	0.73	4	1.36	0.13	7.31	P19397	2 (3)		
CD317	0.96	1	1.04	0.12	0.68	18.90	Q10589	5 (12)		SCAMP1	0.68	4	1.48	0.68	11.80	O15126	2 (5)		
SLC7A1	0.95	14	1.05	0.39	0.56	7.95	P30825	5 (8)		CXCR4 (CD184) ^a	0.56	7	1.80	0.18	3.40	P61073	1 (2)		
SLC1A3/EEA1 ^a	0.95	6	1.06	0.46	0.55	2.03	P43003	1 (2)		HLA-E	0.55	1	1.82	1.19	10.90	P13747	3 (4)		
Flotillin1	0.95	0	1.06	0.45	0.55	63.00	O75955	30 (49)	158	PLP2	0.55	4	1.83	NA	18.40	Q04941	2 (1)		
CD29	0.93	1	1.07	0.19	0.55	10.03	P05556	7 (9)											
Syntaxin4	0.93	1	1.07	0.59	0.55	26.90	Q12846	4 (5)											

^a A protein identified by a single peptide only; for MS/MS spectra see supplemental data.

FIG. 3. Confirmation of mass spectrometry-identified candidates by flow cytometry. *A* and *B*, the change in cell surface expression of novel MARCH9 targets as identified by mass spectrometry was tested by flow cytometry. MARCH9-transduced Sultan B cells (generated as in Fig. 1) were stained for surface expression of the indicated markers. The -fold down-regulation is shown within each dot plot. *B*, the change in MHC class II expression in Sultan B cells was compared between MARCH9- (*upper panel*) and MARCH1- (*lower panel*)-transduced Sultan B cells. *C*, alignment of the transmembrane region and cytoplasmic tails of MHC class II (HLA-DQ, -DR, and -DP) chains. The transmembrane regions (*underlined*) and the cytoplasmic tails of class II α and β chains were aligned. Amino acids that are identical to those in HLA-DQ are shaded.



using SILAC (24), we used a 2-fold cutoff that identifies the stronger targets of MARCH9 such as ICAM-1 and Fc γ RIIB, which showed a 2.3- and 3.6-fold down-regulation, respectively. In total, 12 plasma membrane proteins displayed changes above this threshold (Table I and Fig. 2B). These include three receptor-type tyrosine phosphatases, PTPRA (8.2-fold down; based on six different peptides), PTPRJ (CD148) (3.2-fold; 17 peptides), and PTPRF (2.5-fold; one peptide); the antigen-presenting molecule HLA-DQA (2.1-fold; 5 peptides) and -DQB chain (2.5-fold; 12 peptides) but not the closely related HLA-DR (unchanged; >10 peptides) or HLA-DP (unchanged; >10 peptides); the costimulatory molecule SLAM (CD150) (4.7-fold; three peptides); the inhibitory receptor ILT-2 (CD85j, LIR, or LILRB1) (2.3-fold; three peptides); the Fc receptor-related molecule FCRL2 (2-fold; two peptides); plexin C1/CD232 (2-fold; four peptides), an inhibi-

tor of integrin-mediated adhesion of dendritic cells; the soluble N-ethylmaleimide-sensitive factor attachment protein receptor VAMP8 (2.4-fold; six peptides) involved in endocytic vesicle fusion; and a protein of unknown function, TMEM2 (2.2-fold; two peptides). No peptides specific for IgD were identified, but five peptides mapping to the closely related IgM gave a 1.7-fold change that would have been considered borderline without the previous identification of IgD as a potential substrate. No specific peptides for PVR were detected.

Validation of Novel MARCH9 Substrates by Flow Cytometry—Monoclonal antibodies were available for six of the 12 MARCH9 targets identified (ICAM-1, Fc γ RIIB, SLAM, PTPRJ, ILT-2, and HLA-DQ), allowing us to validate the SILAC MS/MS results using an alternative technique. By flow cytometric analysis we confirmed a marked decrease in cell surface expression of all six targets (Fig. 3). In these experiments

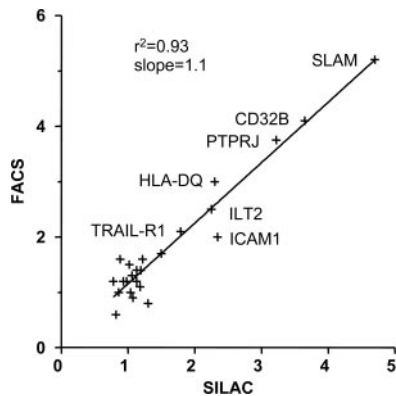


FIG. 4. The -fold down-regulation of novel targets identified by SILAC MS correlates with flow cytometry. The -fold down-regulation of all targets identified by both SILAC MS and flow cytometry is compared. Regression analysis shows a linear correlation with a correlation coefficient (r^2) of 0.93. The data points of the proteins displaying a change in expression levels are annotated. FACS, fluorescence-activated cell sorting.

MARCH1-overexpressing Sultan cells served as a control. MARCH1 is a related RING-CH E3 ligase, also expressed in B cells, that down-regulates MHC class II as well as B7.2 (16). Although MARCH1 does not discriminate between MHC class II molecules, MARCH9, as originally shown by mass spectrometry, only down-regulated HLA-DQ leaving both HLA-DR and HLA-DP unaffected (Fig. 3B).

SLAM (CD150), the principal measles virus receptor, is a costimulatory molecule expressed on lymphocytes and mature dendritic cells (25). SLAM was strongly reduced by MARCH9 as was expression of the protein-tyrosine phosphatase receptor PTPRJ (CD148) (Fig. 3A). ILT-2 (CD85j, LIR, or LILRB1), one of nine members of the family of Ig-like receptors for MHC class I, was identified by a single peptide also mapping to the closely related ILT-4, but only ILT-2 is expressed on B cells (26). The expression of ILT-2 was significantly reduced in the presence of MARCH9. We also analyzed TRAIL-R1 (CD261, TNFR10A), which was only reduced 1.8-fold by SILAC and showed a corresponding small effect by flow cytometry (Fig. 3A).

We wanted to determine how the change in cell surface expression of proteins detected by mass spectrometry correlated with flow cytometry, the gold standard for quantitative analysis of cell surface receptor expression. The -fold change in expression levels for all proteins detected by both mass spectrometry and flow cytometry was therefore compared (Fig. 4). This analysis allows a direct assessment of the correlation and therefore the quality of the mass spectrometry data. The correlation coefficient of 0.93 indicates a remarkably strong correlation between the two methodologies.

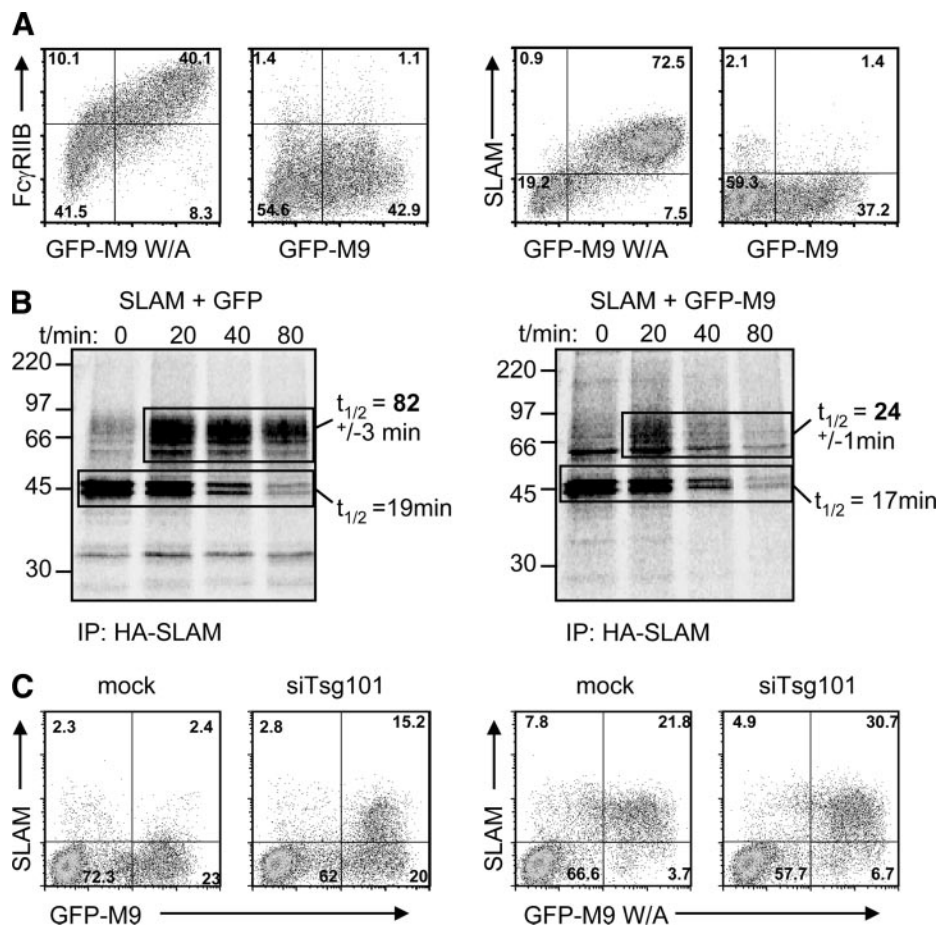
Mechanism of Down-regulation—The specific reduction of HLA-DQ but not HLA-DR or HLA-DP suggested that MARCH9-mediated down-regulation is a post-transcriptional event because transcription of all three MHC class II alleles is

controlled by the same master regulator, the MHC class II transactivator encoded by the gene AIR-1 (activator of immune response locus 1) (CIITA). This differential HLA-DQ down-regulation by MARCH9 was also seen in HeLa cells expressing CIITA (data not shown). We previously showed that MARCH9 ubiquitinates and down-regulates ICAM-1 and requires the lysine residues in the cytosolic tail of ICAM-1. To determine whether some of the newly identified substrates were also dependent on the E3 ligase activity of MARCH9, we first showed that expression of a MARCH9-GFP fusion protein in 293T cells also down-regulated exogenously expressed SLAM and Fc γ RIIB (Fig. 5A). Transfection of the same cells with a mutant MARCH9-GFP fusion construct containing a previously characterized tryptophan to alanine mutation in the K3 RING-CH domain that prevents E2 binding (12, 27) no longer down-regulated Fc γ RIIB or SLAM surface expression. The E3 ligase activity of MARCH9 is therefore required for substrate down-regulation (Fig. 5A).

We wanted to ascertain how the identified receptors were down-regulated in MARCH9-expressing cells and concentrated on SLAM, a MARCH9 target that could be followed in 293T as well as Sultan cells. A pulse-chase analysis of radio-labeled, HA-tagged SLAM in transfected 293T cells was performed followed by immunoprecipitation of HA-tagged SLAM (Fig. 5B). To distinguish immature, ER-resident SLAM from proteins that had trafficked through the secretory pathway, samples were incubated with Endo H, which cleaves only immature glycans. Human SLAM has eight putative glycosylation sites for N-linked glycans of which seven are conserved in the murine ortholog. Following treatment of murine SLAM with N-glycosidase F, which cleaves all glycans, the molecular mass is reduced from 70 to 45 kDa (28). We saw a similar collapse for Endo H-treated immature human SLAM molecules (from over 60 to 45 kDa; data not shown). We used this marker to determine how MARCH9 affects the half-life of both immature ER-resident (Endo H-sensitive) SLAM as well as the mature (Endo H-resistant) protein (Fig. 5B). At the start of the chase (time point 0) the majority (85%) of the SLAM was still in the ER and therefore Endo H-sensitive. Immature, Endo H-sensitive SLAM molecules were quickly processed into the mature form, resulting in a half-life of the immature form of 19 min, whereas the half-life of the mature, Endo H-resistant form was 82 min. In the presence of MARCH9 the half-life of immature SLAM was essentially unchanged at 17 min, whereas the half-life of the mature SLAM protein decreased to 24 min. Therefore, in MARCH9-expressing cells, SLAM traffics normally through the ER to the late secretory pathway where it is degraded.

The localization of MARCH9 to lysosomes suggests a role in lysosomal degradation of receptor proteins (18). Tsg101 is a critical component of the endosomal sorting complex required for transport (ESCRT) pathway involved in the recognition of ubiquitinated cargo for delivery to multivesicular bodies for endolysosomal degradation (41). We therefore

FIG. 5. Mechanism of substrate down-regulation. A, Fc γ RIIB or SLAM were co-transfected together with GFP-tagged wild-type or tryptophan to alanine mutant (W/A) MARCH9 into 293T cells and stained with antibodies specific for Fc γ RIIB or SLAM. The percentage of cells in each quadrant is shown. B, pulse-chase analysis of metabolically labeled HA-tagged SLAM in the presence or absence of MARCH9. HA-tagged SLAM-expressing 293T cells in the presence or absence of MARCH9 were [35 S]methionine-radiolabeled for 20 min and chased for the times indicated. Triton X-100 lysates were immunoprecipitated with HA-specific monoclonal antibody and treated with Endo H. Samples were analyzed by SDS-PAGE and autoradiography. The half-life ($t_{1/2}$) of the Endo H-sensitive, immature form and the Endo H-resistant, mature form of SLAM is shown. C, Tsg101 siRNA-depleted 293T cells were co-transfected with SLAM and GFP-tagged MARCH9. SLAM and MARCH9 expression were analyzed by flow cytometry and compared with mock-depleted cells or cells transfected with tryptophan to alanine mutant MARCH9 (W/A). IP, immunoprecipitation.



assessed the role of Tsg101 in MARCH9-mediated SLAM down-regulation. 293T cells were depleted of Tsg101 by siRNA and subsequently co-transfected with GFP-tagged wild-type or RING tryptophan to alanine mutant MARCH9 and SLAM (Fig. 5C). Following Tsg101 depletion, SLAM expression was restored at the cell surface in the MARCH9 (GFP-positive) population. In the presence of the MARCH9 tryptophan to alanine RING mutant, SLAM remained well expressed at the cell surface and was unaffected by Tsg101 depletion. Taken together these results suggest that MARCH9-mediated SLAM down-regulation occurs in the late secretory pathway and that SLAM is degraded via an endolysosomal pathway.

DISCUSSION

SILAC has emerged as a popular and powerful technique for quantitative proteomics. A major advantage of SILAC is that the *in vivo* incorporation of heavy isotopes, with the resulting mass shift in corresponding peptides, allows the mixing of test and control samples immediately after cell harvesting and prior to any fractionation procedure. This critical step minimizes the inherent errors in sample preparation, particularly those procedures requiring multiple steps such as organelle purification. In this study we used SILAC to identify plasma membrane proteins that are differentially expressed in

the presence of the MARCH9 E3 ligase and therefore represent potential new MARCH9 substrates. The combination of mass spectrometry to identify the novel cell surface target proteins with subsequent validation by flow cytometry proved to be effective. The close correlation ($r^2 = 0.93$) in receptor down-regulation as measured by SILAC and flow cytometry emphasizes the reliability of the quantitative mass spectrometry data (Fig. 4).

MARCH9 is a membrane-bound ubiquitin E3 ligase that can regulate expression of an increasing number of plasma membrane receptors. We identified 13 novel plasma membrane proteins whose expression was decreased in the presence of MARCH9 (Table II). Flow cytometry initially identified three new candidate substrates with decreased expression on the surface of MARCH9-expressing cells and has the advantage of being sensitive and easily reproducible but requires a large set of antibodies and remains therefore cost-prohibitive (Fig. 1B). The quantitative proteomics analysis identified over 900 proteins of which 157 (16%) were plasma membrane proteins according to UniProt annotations. Twelve of these proteins showed at least a 2-fold reduction in expression in the presence of MARCH9 (Table I). All six of the potential MARCH9 substrates for which monoclonal antibodies were available (Fc γ RIIB (CD32B), ICAM-1

TABLE II
Targets identified by flow cytometry and SILAC MS/MS

CD numbers and -fold down-regulation as measured by SILAC are given in parentheses. ND, no data available. Confirmed, SILAC MS/MS-identified targets that were subsequently confirmed by flow cytometry. Note that HLA-DQ is listed twice as α and β chain (numbers 8a and 8b). Changes in expression of 2-fold or more are highlighted in bold.

No.	Flow cytometry	SILAC MS/MS
1	ICAM-1 (CD54)	ICAM-1 (CD54; 2.3 \times)
2	FcγRIIB (CD32)	FcγRIIB (CD32; 3.7 \times)
3	PVR (CD155)	ND
4	IgD	ND
5	ND	PTPRA (8.2 \times)
6	Confirmed	SLAM (CD150; 4.7 \times)
7	Confirmed	PTPRJ (CD148; 3.7 \times)
8a	Confirmed	HLA-DQB (2.5 \times)
8b	Confirmed	HLA-DQA (2.1 \times)
9	ND	PTPRF (2.5 \times)
10	ND	VAMP8 (2.4 \times)
11	Confirmed	ILT-2 (CD85j; 2.3 \times)
12	ND	TMEM2 (2.2 \times)
13	ND	Plexin C1 (2.0 \times)
14	ND	FCRL2 (2.0 \times)

(CD54), ILT-2 (CD85j), PTPRJ (CD148), SLAM (CD150), and HLA-DQ) were confirmed by flow cytometry as being decreased in MARCH9-expressing cells (Fig. 3).

Among the 13 novel substrates of MARCH9 are several interesting candidates. Of greatest significance are those receptors that were well expressed and showed the greatest down-regulation. These include four proteins (PTPRJ, SLAM, Fc γ RIIB, and HLA-DQ), all of which showed at least a 3-fold change in expression by flow cytometry.

A role for ubiquitin in receptor regulation is well characterized for the receptor tyrosine kinases, as exemplified by the epidermal growth factor receptor (10), but to our knowledge this has not been reported for receptor tyrosine phosphatases. Substrate-induced phosphorylation of EGFR not only initiates signaling but also recruits the Cbl ubiquitin E3 ligase that terminates signaling by binding and ubiquitinating its target receptor and in the case of EGFR promotes internalization and endosomal sorting for lysosomal degradation. Receptor protein-tyrosine phosphatases such as PTPRJ (CD148) and PTPRC (CD45) play an important regulatory role in T and B cell signaling where they activate Src family kinases by dephosphorylating the inhibitory tyrosine in the tail of the kinase (29). PTPRA, also an activator of Src family kinases (30), showed the strongest down-regulation by MS, giving an 8-fold change with a narrow standard deviation from six different peptides. PTPRF is the third member of this family affected by MARCH9 but represents a weak hit as it was only identified by a single peptide and, like PTPRA, lacks an antibody for confirmation by flow cytometry. Although little is known about the regulation of the protein receptor tyrosine phosphatases, the important role of PTPRJ (CD148) and other

tyrosine phosphatases in B and T cell signaling suggests that their regulation by E3 ligases could be of major significance.

One of the most marked differences in cell surface expression induced by MARCH9 was seen with SLAM (CD150), a costimulatory molecule expressed on lymphocytes (for a review, see Ref. 25). SLAM stimulation supports B cell proliferation and differentiation (31), whereas the SLAM knock-out mouse shows a reduction in IL-4 secretion by T cells and impaired macrophage function (32). SLAM triggers tyrosine phosphorylation via interaction with an adaptor molecule, SAP, which recruits the Src-related protein-tyrosine kinase FynT. The SLAM/SAP pathway plays an essential role in the development of the innate immune system, in particular NKT cells. Lack of SAP leads to NKT cell deficiency and a dysregulation of immune responses exemplified by the X-linked lymphoproliferative disorder. SAP is also essential for T cell function as SAP-deficient CD4⁺ T cells show a reduced ability to stimulate B cells, whereas CD8⁺ T cells are defective in cytolytic granule secretion. In this regard, the reduced expression of the vesicle-associated membrane protein VAMP8 in MARCH9-expressing cells is of interest as VAMP8 is an important mediator of endosomal vesicle fusion and regulated granule secretion (33–35).

The basis of substrate selection and specificity by MARCH9 is not understood. Studies of other RING-CH proteins have shown a requirement for substrate interactions within the membrane. MARCH9 carries a charged residue (aspartate) in its second transmembrane region, which partially inhibits down-regulation of MHC-I, supporting a role for this region in target identification (18). The situation appears more complex with respect to HLA-DQ, another newly identified MARCH9 target. Although the related MARCH1 and MARCH8 E3 ligases down-regulate all three MHC class II alleles (HLA-DP, -DQ, and -DR) MARCH9 had an unanticipated effect on decreasing cell surface expression of HLA-DQ alone with no effect on HLA-DP or -DR. The transmembrane regions of the HLA-DQ heterodimer (HLA-DQ α and -DQ β) are almost identical to those of HLA-DR (HLA-DR α and -DR β) (Fig. 3C) and are unlikely to be the discriminating factor for HLA-DQ down-regulation. HLA-DQ may represent an indirect target of MARCH9, *i.e.* an example where MARCH9 down-regulates an upstream target whose expression is required for HLA-DQ. HLA-DQ expression does require an unidentified additional cellular cofactor as interspecies somatic cell hybrids of the AIR-1 (class II transactivator)-defective human B cell line RJ 2.2.5 with mouse B cells rescues the surface expression of HLA-DR and -DP but not HLA-DQ despite normal expression of HLA-DQ transcripts (36, 37). Whether HLA-DQ or its predicted cofactor is the true target of MARCH9 needs to be determined.

The fourth potential target identified by quantitative mass spectrometry as well as flow cytometry is the Fc γ RIIB (CD32B). Fc γ RIIB is the only inhibitory Fc receptor for IgG and plays an important role in regulation of B cell receptor signal-

ing (38). IgD, which showed a strong down-regulation by flow cytometry (Fig. 1B), is the antigen-binding part of the B cell receptor (39) and the only component that could be detected at satisfactory levels by flow cytometry. Whether there is a connection between the down-regulation of Fc γ RIIB and IgD remains to be investigated.

MARCH9 is expressed in lysosomal compartments (18), and degradation of a previously identified MARCH9 substrate occurred via a lysosomal pathway (11). For two of the newly identified targets (Fc γ RIIb and SLAM), down-regulation was dependent on E3 ligase activity as a mutant RING, which is unable to recruit an E2-conjugating enzyme, did not cause receptor down-regulation (Fig. 5A). Further examination of the SLAM protein showed that only Endo H-resistant forms were degraded in the presence of MARCH9 with a 3.4-fold reduction in half-life of Endo H-resistant SLAM and no effect on Endo H-sensitive SLAM (Fig. 5B). For this receptor, as for the few other receptors examined (11), MARCH9 does not use endoplasmic reticulum-associated protein degradation but causes substrate degradation in the late secretory pathway. This was confirmed by depleting cells of Tsg101, a critical component of the ESCRT1 complex (41). We previously showed that depletion of Tsg101 inhibits the K3-dependent, lysosomal degradation of MHC class I (40), and Tsg101 depletion also rescued cell surface SLAM expression in MARCH9-expressing cells (Fig. 5C). SLAM expression was not increased above steady state levels in cells expressing the RING tryptophan to alanine mutant form of MARCH9, suggesting that Tsg101 depletion in MARCH9-expressing cells causes SLAM to recycle back to the cell surface. Therefore, in the presence of MARCH9, SLAM is degraded via an endolysosomal route, although this needs to be confirmed for other MARCH9 substrates.

The plasma membrane remains a challenging compartment to purify, and using the modified form of the colloidal silica technique we identified 157 plasma membrane proteins (including 145 transmembrane proteins). Despite extensive washing with carbonate buffer, we still had a substantial contamination mainly from abundant cytosolic and nuclear proteins. However, only one (DHX29) of the ~800 non-plasma membrane proteins identified by at least two peptides showed a significant decrease in the presence of MARCH9. This result substantiates our initial assumption that MARCH9 predominantly targets membrane proteins. One of the cytoplasmic proteins, SH3BP1, displayed a significant change in expression (6.8-fold down), but this was only seen on a single peptide. SH3BP1 is a member of the GTPase-activating protein family interacting with and inactivating plasma membrane-bound Rho GTPases. If confirmed, this down-regulation might represent an example of an indirect effect caused by down-regulation of the unspecified interaction partner at the membrane. A few cytosolic, mitochondrial, and nuclear proteins appeared to be up-regulated in the presence of MARCH9, but on closer inspection many of these turned out

to be based on single peptide identifications or outliers resulting in a high standard deviation (see supplemental data). One interesting exception is Hu antigen R (ELAV1), an mRNA stabilizing factor that was ~2.5-fold up-regulated. It remains to be investigated whether that is a response of the cell to the degradative effect of MARCH9.

Recently Bartee *et al.* (22) took a similar approach, isolating different membrane fractions from SILAC-labeled HeLa cells to identify novel substrates of the viral E3 ligase K5. K5 is related to the MARCH family and is reported to down-regulate both ER as well as plasma membrane proteins. Following the enrichment of ER, Golgi apparatus, and plasma membrane fractions three novel K5 substrates were identified, including activated lymphocyte cell adhesion molecule (CD166), which they showed to also be down-regulated by MARCH9. Direct comparison of the two studies is difficult, but the combined experience suggests that SILAC is particularly powerful for examination of enriched individual organelles rather than the whole membrane fraction. Five of the confirmed targets of MARCH9 are exclusively expressed in immune cells, and additional targets might be identified in other cell types.

Our comparative analysis of the plasma membrane proteome identified new potential targets of MARCH9 and provided important candidate substrates to help elucidate the physiological role of this poorly characterized E3 ligase. The quantitative mass spectrometry of plasma membrane proteins by SILAC proved a powerful technique to identify alterations in cell surface receptor abundance. The rapid validation of the new finds by flow cytometry makes this a particularly attractive approach. The same methodology can be applied to determine the effect of other host- or pathogen-derived gene products on plasma membrane receptor expression as well as to quantify changes in receptor expression during cellular activation or differentiation.

Acknowledgments—We thank the Smoler Proteomics Centre at the Technion Institute in Haifa for excellent technical support, Chris Richardson for SLAM expression constructs, and Andres Floto for CD32 constructs.

* This work was supported by the Wellcome Trust and Cambridge University Hospitals Biomedical Research Centre.

§ The on-line version of this article (available at <http://www.mcponline.org>) contains supplemental material.

¶ A Lister Prize Fellow. To whom correspondence should be addressed: Cambridge Inst. for Medical Research, University of Cambridge, Addenbrooke's Hospital, Hills Rd., Cambridge CB2 0XY, UK. Tel.: 44-1223-762113; Fax: 44-1223-762640; E-mail: pjl30@cam.ac.uk.

REFERENCES

1. Staub, O., and Rotin, D. (2006) Role of ubiquitylation in cellular membrane transport. *Physiol. Rev.* **86**, 669–707
2. Liu, Y. C. (2004) Ubiquitin ligases and the immune response. *Annu. Rev. Immunol.* **22**, 81–127
3. Zola, H., Swart, B., Banham, A., Barry, S., Beare, A., Bensussan, A., Boumsell, L., Buckley, C. D., Bühring, H. J., Clark, G., Engel, P., Fox, D., Jin, B. Q., Macardle, P. J., Malavasi, F., Mason, D., Stockinger, H., and

- Yang, X. (2007) CD molecules 2006–human cell differentiation molecules. *J. Immunol. Methods* **319**, 1–5
4. Arkin, I. T., and Brunger, A. T. (1998) Statistical analysis of predicted transmembrane alpha-helices. *Biochim. Biophys. Acta* **1429**, 113–128
 5. Naramura, M., Jang, I. K., Kole, H., Huang, F., Haines, D., and Gu, H. (2002) c-Cbl and Cbl-b regulate T cell responsiveness by promoting ligand-induced TCR down-modulation. *Nat. Immunol.* **3**, 1192–1199
 6. Pickart, C. M. (2001) Mechanisms underlying ubiquitination. *Annu. Rev. Biochem.* **70**, 503–533
 7. Mori, S., Heldin, C. H., and Claesson-Welsh, L. (1993) Ligand-induced ubiquitination of the platelet-derived growth factor beta-receptor plays a negative regulatory role in its mitogenic signaling. *J. Biol. Chem.* **268**, 577–583
 8. Galcheva-Gargova, Z., Theroux, S. J., and Davis, R. J. (1995) The epidermal growth factor receptor is covalently linked to ubiquitin. *Oncogene* **11**, 2649–2655
 9. Huang, F., Kirkpatrick, D., Jiang, X., Gygi, S., and Sorkin, A. (2006) Differential regulation of EGF receptor internalization and degradation by multiubiquitination within the kinase domain. *Mol. Cell* **21**, 737–748
 10. Levkowitz, G., Waterman, H., Zamir, E., Kam, Z., Oved, S., Langdon, W. Y., Beguinot, L., Geiger, B., and Yarden, Y. (1998) c-Cbl/Sli-1 regulates endocytic sorting and ubiquitination of the epidermal growth factor receptor. *Genes Dev.* **12**, 3663–3674
 11. Bartee, E., Mansouri, M., Hovey Nerenberg, B. T., Gouveia, K., and Früh, K. (2004) Downregulation of major histocompatibility complex class I by human ubiquitin ligases related to viral immune evasion proteins. *J. Virol.* **78**, 1109–1120
 12. Dodd, R. B., Allen, M. D., Brown, S. E., Sanderson, C. M., Duncan, L. M., Lehner, P. J., Bycroft, M., and Read, R. J. (2004) Solution structure of the Kaposi's sarcoma-associated herpesvirus K3 N-terminal domain reveals a Novel E2-binding C4HC3-type RING domain. *J. Biol. Chem.* **279**, 53840–53847
 13. Lehner, P. J., Hoer, S., Dodd, R., and Duncan, L. M. (2005) Downregulation of cell surface receptors by the K3 family of viral and cellular ubiquitin E3 ligases. *Immunol. Rev.* **207**, 112–125
 14. Ohmura-Hoshino, M., Goto, E., Matsuki, Y., Aoki, M., Mito, M., Uematsu, M., Hotta, H., and Ishido, S. (2006) A novel family of membrane-bound E3 ubiquitin ligases. *J. Biochem.* **140**, 147–154
 15. Ohmura-Hoshino, M., Matsuki, Y., Aoki, M., Goto, E., Mito, M., Uematsu, M., Kakiuchi, T., Hotta, H., and Ishido, S. (2006) Inhibition of MHC class II expression and immune responses by c-MIR. *J. Immunol.* **177**, 341–354
 16. Matsuki, Y., Ohmura-Hoshino, M., Goto, E., Aoki, M., Mito-Yoshida, M., Uematsu, M., Hasegawa, T., Koseki, H., Ohara, O., Nakayama, M., Toyooka, K., Matsuoka, K., Hotta, H., Yamamoto, A., and Ishido, S. (2007) Novel regulation of MHC class II function in B cells. *EMBO J.* **26**, 846–854
 17. Su, A. I., Cooke, M. P., Ching, K. A., Hakak, Y., Walker, J. R., Wiltshire, T., Orth, A. P., Vega, R. G., Sapinoso, L. M., Moqrich, A., Patapoutian, A., Hampton, G. M., Schultz, P. G., and Hogenesch, J. B. (2002) Large-scale analysis of the human and mouse transcriptomes. *Proc. Natl. Acad. Sci. U.S.A.* **99**, 4465–4470
 18. Hoer, S., Smith, L., and Lehner, P. J. (2007) MARCH-IX mediates ubiquitination and downregulation of ICAM-1. *FEBS Lett.* **581**, 45–51
 19. Ong, S. E., Blagoev, B., Kratchmarova, I., Kristensen, D. B., Steen, H., Pandey, A., and Mann, M. (2002) Stable isotope labeling by amino acids in cell culture, SILAC, as a simple and accurate approach to expression proteomics. *Mol. Cell. Proteomics* **1**, 376–386
 20. Chaney, L. K., and Jacobson, B. S. (1983) Coating cells with colloidal silica for high yield isolation of plasma membrane sheets and identification of transmembrane proteins. *J. Biol. Chem.* **258**, 10062–10072
 21. Rahbar, A. M., and Fenselau, C. (2004) Integration of Jacobson's pellicle method into proteomic strategies for plasma membrane proteins. *J. Proteome Res.* **3**, 1267–1277
 22. Bartee, E., McCormack, A., and Früh, K. (2006) Quantitative membrane proteomics reveals new cellular targets of viral immune modulators. *PLoS Pathog.* **2**, e107
 23. Tomasec, P., Wang, E. C., Davison, A. J., Vojtesek, B., Armstrong, M., Griffin, C., McSharry, B. P., Morris, R. J., Llewellyn-Lacey, S., Rickards, C., Nomoto, A., Sinzger, C., and Wilkinson, G. W. (2005) Downregulation of natural killer cell-activating ligand CD155 by human cytomegalovirus UL141. *Nat. Immunol.* **6**, 181–188
 24. Ong, S. E., Foster, L. J., and Mann, M. (2003) Mass spectrometric-based approaches in quantitative proteomics. *Methods* **29**, 124–130
 25. Veillette, A., Dong, Z., and Latour, S. (2007) Consequence of the SLAM-SAP signaling pathway in innate-like and conventional lymphocytes. *Immunity* **27**, 698–710
 26. Colonna, M., Nakajima, H., Navarro, F., and López-Botet, M. (1999) A novel family of Ig-like receptors for HLA class I molecules that modulate function of lymphoid and myeloid cells. *J. Leukoc. Biol.* **66**, 375–381
 27. Cao, Z., Huett, A., Kuballa, P., Giallourakis, C., and Xavier, R. J. (2008) DLG1 is an anchor for the E3 ligase MARCH2 at sites of cell-cell contact. *Cell. Signal.* **20**, 73–82
 28. Castro, A. G., Hauser, T. M., Cocks, B. G., Abrams, J., Zurawski, S., Churakova, T., Zonin, F., Robinson, D., Tangye, S. G., Aversa, G., Nichols, K. E., de Vries, J. E., Lanier, L. L., and O'Garra, A. (1999) Molecular and functional characterization of mouse signaling lymphocytic activation molecule (SLAM): differential expression and responsiveness in Th1 and Th2 cells. *J. Immunol.* **163**, 5860–5870
 29. Zhu, J. W., Brdicka, T., Katsumoto, T. R., Lin, J., and Weiss, A. (2008) Structurally distinct phosphatases CD45 and CD148 both regulate B cell and macrophage immunoreceptor signaling. *Immunity* **28**, 183–196
 30. Pallen, C. J. (2003) Protein tyrosine phosphatase alpha (PTPalph): a Src family kinase activator and mediator of multiple biological effects. *Curr. Top. Med. Chem.* **3**, 821–835
 31. Punnonen, J., Cocks, B. G., Carballido, J. M., Bennett, B., Peterson, D., Aversa, G., and de Vries, J. E. (1997) Soluble and membrane-bound forms of signaling lymphocytic activation molecule (SLAM) induce proliferation and Ig synthesis by activated human B lymphocytes. *J. Exp. Med.* **185**, 993–1004
 32. Wang, N., Satoskar, A., Faubion, W., Howie, D., Okamoto, S., Feske, S., Gullo, C., Clarke, K., Sosa, M. R., Sharpe, A. H., and Terhorst, C. (2004) The cell surface receptor SLAM controls T cell and macrophage functions. *J. Exp. Med.* **199**, 1255–1264
 33. Polgár, J., Chung, S. H., and Reed, G. L. (2002) Vesicle-associated membrane protein 3 (VAMP-3) and VAMP-8 are present in human platelets and are required for granule secretion. *Blood* **100**, 1081–1083
 34. Lippert, U., Ferrari, D. M., and Jahn, R. (2007) Endobrevin/VAMP8 mediates exocytotic release of hexosaminidase from rat basophilic leukaemia cells. *FEBS Lett.* **581**, 3479–3484
 35. Wang, C. C., Shi, H., Guo, K., Ng, C. P., Li, J., Gan, B. Q., Chien Liew, H., Leinonen, J., Rajaniemi, H., Zhou, Z. H., Zeng, Q., and Hong, W. (2007) VAMP8/endobrevin as a general vesicular SNARE for regulated exocytosis of the exocrine system. *Mol. Biol. Cell* **18**, 1056–1063
 36. Accolla, R. S., Tosi, G., Sartoris, S., and De Lerma Barbaro, A. (1999) MHC class II gene regulation: some historical considerations on a still ontogenetic and phylogenetic puzzle. *Microbes Infect.* **1**, 871–877
 37. De Lerma Barbaro, A., Sartoris, S., Tosi, G., Nicolis, M., and Accolla, R. S. (1994) Evidence for a specific post-transcriptional mechanism controlling the expression of HLA-DQ, but not -DR and -DP, molecules. *J. Immunol.* **153**, 4530–4538
 38. Nimmerjahn, F., and Ravetch, J. V. (2006) Fcγ receptors: old friends and new family members. *Immunity* **24**, 19–28
 39. Matsuuchi, L., and Gold, M. R. (2001) New views of BCR structure and organization. *Curr. Opin. Immunol.* **13**, 270–277
 40. Hewitt, E. W., Duncan, L., Mufti, D., Baker, J., Stevenson, P. G., and Lehner, P. J. (2002) Ubiquitylation of MHC class I by the K3 viral protein signals internalization and TSG101-dependent degradation. *EMBO J.* **21**, 2418–2429
 41. Bishop, N., Horman, A., and Woodman, P. (2002) Mammalian class E vps proteins recognize ubiquitin and act in the removal of endosomal protein-ubiquitin conjugates. *J. Cell Biol.* **157**, 91–101